An X-Ray-selected Active Galactic Nucleus at z=4.6 Discovered by the CYDER Survey

Treister, E.; Castander, F.J.; Maccarone, T.J.; Herrera, D.; Gawiser, E.; Maza, J.; Coppi, P.S.

DOI
10.1086/381432

Publication date
2004

Published in
Astrophysical Journal

The Astrophysical Journal, 603:36–41, 2004 March 1

AN X-RAY–SELECTED ACTIVE GALACTIC NUCLEUS AT $z = 4.6$ DISCOVERED BY THE CYDER SURVEY[1]

Ezequiel Treister,[2,3] Francisco J. Castander,[4] Thomas J. Maccarone,[5] David Herrera,[2] Eric Gawiser,[2,3,6] José Maza,[2] and Paolo S. Coppi[1]

Received 2003 October 8; accepted 2003 November 17

ABSTRACT

We present the discovery of a high-redshift, X-ray–selected active galactic nucleus (AGN) by the Calan-Yale Deep Extragalactic Research (CYDER) survey: CXOCY J033716.7−050153, located at $z = 4.61$, the second high-redshift AGN discovered by this survey. Here we present its optical, near-IR, and X-ray properties and compare it with other optical and X-ray–selected high-redshift AGNs. The optical luminosity of this object is significantly lower than most optically selected high-redshift quasars. It also has a lower rest-frame UV to X-ray emission ratio than most known quasars at this redshift. This mild deviation can be explained either by dust obscuring the UV radiation of a normal radio-quiet AGN emitting at 10% of its Eddington luminosity or because this is intrinsically a low-luminosity radio-loud AGN with a supermassive black hole of $\sim 10^8\ M_\odot$ emitting at 1% of its Eddington luminosity. Deep radio observations can discriminate between these two hypotheses.

Subject headings: galaxies: active — quasars: individual (CXOCY J033716.7−050153) — X-rays: galaxies

1. INTRODUCTION

Because of its large intrinsic luminosity, an active galactic nucleus (AGN) can be observed up to very high redshifts, and AGNs can therefore be used to probe the early epochs of the universe when the formation of large structures began. Recent observations have found a considerable number of quasars at high redshift (Anderson et al. 2001; Schneider et al. 2002), with some of them at redshift greater than 6 (Fan et al. 2003), when the universe was about 1 Gyr old.

While AGNs were first noticed to be a class of objects worthy of detailed follow-up in other bands on the basis of their radio emission (e.g., Schmidt 1963), more recent work has focused on surveys at shorter wavelengths. Because of their low spatial density, most AGNs at high redshift (defined here to be $z > 4$) were discovered by large-area, shallow optical surveys. An example of this is the Sloan Digital Sky Survey (SDSS; York et al. 2000), which in its first data release (Schneider et al. 2003) presented 238 high-redshift quasars. However, these quasars were selected on the basis of their optical properties, and optical surveys are subject to bias against the discovery of quasars that are either intrinsically dim at these wavelengths or are obscured by dust like the type-2 AGNs that are believed to comprise most of the AGN background (Hasinger 2002).

The other main AGN selection technique is X-ray detection, as X-ray emission appears to be a universal characteristic of AGNs at all observed redshifts (Kaspi et al. 2000). However, given the relative faintness of the majority of the sources, X-ray surveys need to rely on optical spectroscopy for most of the identifications. With new X-ray missions such as the *Chandra X-Ray Observatory* and its superb angular resolution, the identification of X-ray sources at other wavelengths has become much easier, allowing for successful multiwavelength follow-up of X-ray sources. The nature of the X-ray emission also ensures that the optical selection bias due to obscuration is strongly reduced (although the X-ray selection may introduce other biases). This is especially true at high redshift, where the observed X-ray photons were emitted at higher energies and can penetrate even considerable amounts of obscuring material.

According to a recent review by Brandt et al. (2003), only seven of the high-redshift AGNs known were discovered by their X-ray emission. Three of them were found with *ROSAT* (Henry et al. 1994; Zickgraf et al. 1997; Schneider et al. 1998), while the other four were detected by *Chandra* (Silverman et al. 2002; Barger et al. 2002; Castander et al. 2003a). One of them was detected in the radio and classified as radio-loud (Zickgraf et al. 1997).

In this paper we present the discovery of the eighth high-redshift X-ray–selected AGN, and the second discovered by the Calan Yale Deep Extragalactic Research (CYDER) survey, at a redshift $z = 4.61$. The CYDER survey is a collaborative effort between Universidad de Chile and Yale University to study faint stellar and extragalactic populations in detail. One of the key aims is the characterization of the population of faint X-ray sources. In order to do this, some of the fields of the survey were selected to overlap with moderately deep ($\sim$50 ks) *Chandra* pointings. Multiwavelength follow-up in these fields includes optical imaging using the CTIO 4 m telescope, near-IR images obtained using the DuPont Telescope at Las Campanas Observatory (LCO), and optical spectroscopy from VLT at Cerro Paranal and Magellan at LCO. A more complete review of the optical and spectroscopic properties of the X-ray sources in the first two fields can be found in Castander et al. (2003b).

In § 2 we describe the X-ray, optical, and near-IR observations that led to the discovery of the AGN presented here. In § 3 we discuss its observed properties and compare it with

[1] Partly based on observations collected at the European Southern Observatory, Chile, under program 72.A-0509.

[2] Department of Astronomy, Yale University, P.O. Box 208101, New Haven, CT 06520; treister@astro.yale.edu.

[3] Departamento de Astronomía, Universidad de Chile, Casilla 36-D, Santiago, Chile.

[4] Institut d'Estudis Espacials de Catalunya/CSIC, Gran Capità 2-4, E-08034 Barcelona, Spain.

[5] Astronomical Institute "Anton Pannekoek," University of Amsterdam, 1098 SJ Amsterdam, Netherlands.

[6] NSF Astronomy and Astrophysics Postdoctoral Fellow.

other high-redshift quasars, both optical and X-ray–selected. We present our conclusions in § 4. Throughout this paper we assume $H_0 = 70\ h_{70}$ km s^{-1} Mpc^{-1}, $\Omega_m = 0.3$, and $\Omega_\Lambda = 0.7$. These cosmological parameters are consistent with the recent findings by Spergel et al. (2003). We define the photon index Γ as the exponent giving a photon flux density X-ray spectrum $dN/dE \propto E^{-\Gamma}$ in photons cm^{-2} s^{-1} keV^{-1}.

2. OBSERVATIONS AND DATA ANALYSIS

2.1. *X-Ray Data*

As part of the CYDER Survey, five fields observed by *Chandra* and currently available in the archive were downloaded and analyzed using standard techniques with the CIAO package. In this paper we discuss the results for the source CXOCY J033716.7−050153 found in the SBS 0335−05 field. This field was observed by *Chandra* on 2000 September 7 for 60.51 ks (PI: Thuan) and retrieved from the archive by our group. A detailed analysis of the whole sample of X-ray sources detected in these fields will be presented in E. Treister et al., (2004, in preparation).

Reduction of the data included the removal of bad columns and pixels using the guidelines specified on the "ACIS Recipes: Clean the Data" web page and the removal of flaring pixels using the *flagflare* routine. We used the full set of standard event grades (0, 2, 3, 4, 6) and created two images, one from 0.5 to 2.0 keV and one from 2.0 to 8.0 keV. Then we used the WAVDETECT routine from the CIAO package to identify the point sources within these images, checking wavelet scales 1, 2, 4, 8, and 16.

CXOCY J033716.7−050153 was detected in the I2 ACIS CCD. We extract an X-ray spectrum using a minimum of 5 counts per channel from 0.5 to 3.5 keV (i.e., the 20 lowest energy photons), using the *psextract* script. We then fitted the spectrum within XSPEC 11.0 with a power-law model and absorption constrained to the Galactic value of 4.8×10^{20} from the $N_{\rm H}$ tool. This is relatively unconstraining, yielding a spectral index of $\Gamma = 2.0 \pm 0.6$ and observed fluxes of 1.5×10^{-15} and 3.2×10^{-15} ergs s^{-1} cm^{-2}, from 0.5–2 and 0.5–8 keV, respectively. The fit to the X-ray spectrum did not depend on whether the χ^2 or the C-statistic was used, so it is unlikely that large errors were induced by fitting with an insufficient number of photons per bin. The unabsorbed fluxes are approximately 1.8×10^{-15} and 3.5×10^{-15} ergs s^{-1} cm^{-2}, respectively. The errors should be about 30% owing to the statistical error in the count rate and the uncertainties in the best-fitting spectral models. The cumulative histogram of detected X-ray photons is presented in Figure 1.

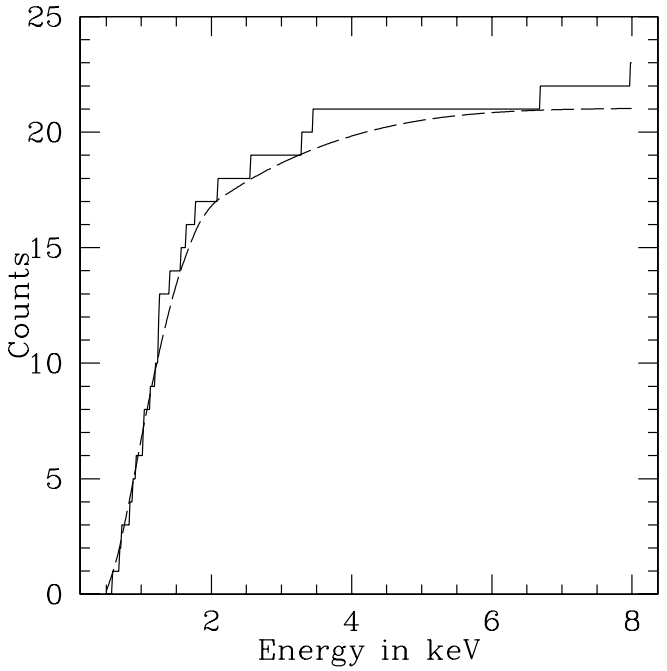

FIG. 1.—Cumulative histogram of detected X-ray photons. The solid line shows the distribution of the data, while the dashed line shows the fitted model with $N_{\rm H} = 4.8 \times 10^{20}$ cm^{-2} and $\Gamma = 2.0$. Errors in the measurement are Poissonian.

2.2. *Optical Imaging Data*

The field of the AGN was observed with the CTIO 4 m Blanco Telescope, using the MOSAIC-II camera, which provides a field of view of $36' \times 36'$. Images were taken using the *B*, *V*, *R*, and *I* filters on the nights of 2002 October 8 and 10, centered on the *Chandra* archival image central coordinates. Exposure times were 2 hr under 1.″3 seeing conditions in the *B* filter, 50 minutes under 1.″1 seeing in *V*, 50 minutes under 1.″1 seeing in *R*, and 20 minutes under 1.″0 seeing in *I*.

A second image in the *I* band was taken with the UT4 VLT telescope at Cerro Paranal, Chile, using the FORS2 instrument. This image was taken on the night of 2003 September 19 in service mode. Total exposure time was 14 minutes under 0.″7 seeing conditions.

Images were reduced using standard techniques with the IRAF/MSCRED package. Identification of the optical counterpart of the X-ray source was straightforward given the superb spatial resolution of the *Chandra Observatory*. Indeed, only one optical source can be found in a 3″ circle around the X-ray emission centroid. The offset between the X-ray and optical positions was less than 0.″1 in right ascension and 0.″5 in declination, In order to calculate the received flux in each band, we performed aperture photometry using an aperture of 1.4 × FWHM of each image, centered on the centroid of the *R* -band source, the band in which the signal-to-noise ratio is highest. The observed magnitudes in each band can be found in Table 1. Figure 2 shows the optical finding chart, based on the *R*-band image.

2.3. *Optical Spectroscopy*

Multislit spectroscopy of X-ray sources detected by *Chandra* in the field of the AGN was obtained at Las Campanas Observatory with the Magellan I (Baade) Telescope, using the LDSS-2 instrument. The observations were taken on the night of 2002 October 4. The field of the high-redshift AGN CXOCY J033716.7−050153 was observed for 2 hr in 0.″75 seeing conditions. The Med/Blue grism was used, giving a dispersion of 5.3 Å pixel^{-1} at a central wavelength of 5500 Å. The obtained spectrum was reduced using standard IRAF tasks called by a customized version of the BOGUS code.[7] We calibrated the wavelength of the spectrum using the He-Ar comparison lamp and the night-sky lines. Rough flux calibration of the spectrum was performed using the spectrum of the LTT9239 spectrophotometric standard.

Figure 3 shows the final, reduced spectrum together with the mean spectrum of quasars at $z > 4$ observed by the SDSS.

[7] Available at http://zwolfkinder.jpl.nasa.gov/~stern/homepage/bogus.html.

TABLE 1
PROPERTIES OF CXOCY J033716.7−050153

Parameter	Value
R.A. (J2000.0) (X-ray)	$03^h37^m16^s.8$
Decl. (J2000.0) (X-ray)	$-05^\circ01'54''.3$
R.A. (J2000.0) (optical)	$03^h37^m16^s.6$
Decl. (J2000.0)(optical)	$-05^\circ01'53''.7$
Galactic N_H[a]	4.8×10^{20} cm^{-2}
z	4.61 ± 0.01
α_{ox}	−1.16 ± 0.16
B magnitude[b]	>26.5
V magnitude[b]	25.76 ± 0.39
R magnitude[b]	24.01 ± 0.08
I magnitude (CTIO)[b]	23.95 ± 0.23
I magnitude (VLT)[b]	23.66 ± 0.07
M_I[c]	−22.14 ± 0.15
$AB_{1450(1+z)}$	23.82
$M_{1450(1+z)}$	−22.45
f_X (0.5–8 keV)	3.5×10^{-15} ergs s^{-1} cm^{-2}
f_X (0.5–2 keV)	1.8×10^{-15} ergs s^{-1} cm^{-2}
L_X (0.5–2 keV)	4.5×10^{44} ergs s^{-1}

[a] Calculated using HEASARC tool *nh*.
[b] AB magnitudes in a 1.4 × FWHM aperture.
[c] Rest-frame *I*-band AB magnitude, assuming the SDSS average quasar spectrum.

Lyα and N v are clearly distinguishable in the spectrum. The measured redshift using these emission lines is $z = 4.61 \pm 0.01$.

3. DISCUSSION

With an absolute magnitude of $M_B = -21.14$ (Vega), calculated extrapolating the *I*-band magnitude using the SDSS QSO composite spectrum (Vanden Berk et al. 2001), CXOCY J033716.7−050153 is a faint AGN. Indeed, there are only two AGNs known at high redshift that are fainter in the optical, VLA J1236+6213 at $z = 4.42$ (Brandt et al. 2001) and CXOHDFN J123719.0+621025 at $z = 4.13$ (Barger et al. 2002), both located in the HDF-N/CDF-N. In X-rays, this quasar shows a luminosity in the [0.5–2.0] keV band of 3.77×10^{44} ergs s^{-1}. This is a large X-ray luminosity for an AGN that is faint in the optical bands. In order to quantify this statement, we can calculate the effective optical to X-ray power-law spectral slope, which is given by

$$\alpha_{ox} = \frac{\log [f_\nu(2\ \mathrm{keV})/f_\nu(2500\,\text{Å})]}{\log [\nu(2\ \mathrm{keV})/\nu(2500\,\text{Å})]}, \quad (1)$$

where f_ν is the flux density per unit of frequency and ν is the frequency of the given wavelength or energy. For this AGN, we measure a value of $\alpha_{ox} = -1.16 \pm 0.16$. The average value for the known sample of $z > 4$ AGNs detected in X-rays[8] is -1.61 ± 0.24 from a total of 71 sources, so this new AGN is a $\sim 2\ \sigma$ deviation. With the data available now we cannot calculate the contribution from the host galaxy to the optical luminosity, but it can only be significant if its luminosity is $\gtrsim 3L_*$. Furthermore, a significant contribution from the host galaxy will only make the optical luminosity of the AGN be smaller, therefore increasing the value of α_{ox} and making the deviation from a typical AGN at this redshift to be even larger.

A plot of α_{ox} as a function of redshift for all the high-redshift AGNs detected in X-rays can be found in Figure 4, and the F_X/F_{UV} relation for these objects is presented in Figure 5. In Figure 4 we can see that the X-ray–selected

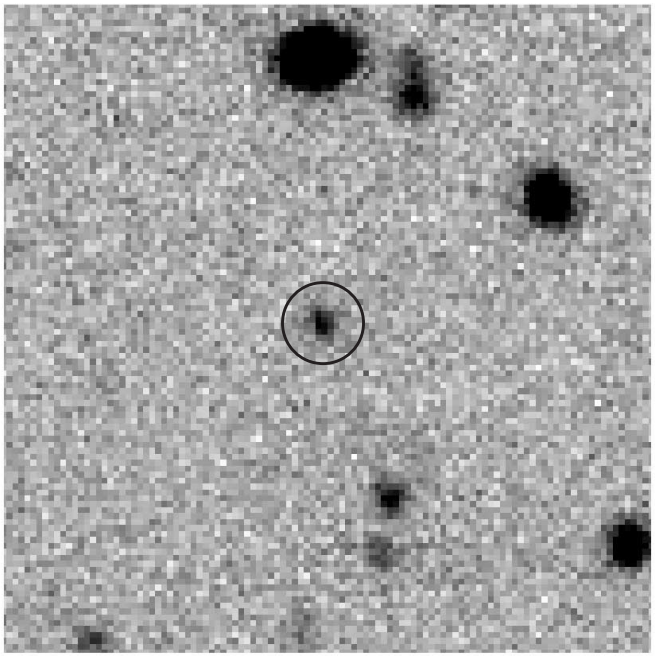

FIG. 2.—*R*-band image of CXOCY J033716.7−050153. This image is a cutout of $30'' \times 30''$ of the original image, centered on the position of the optical counterpart of the X-ray source. North is up, and east is to the left. This image was taken at the CTIO 4 m telescope using the MOSAIC-II camera. A $2''$ circle centered on the optical counterpart position is also plotted.

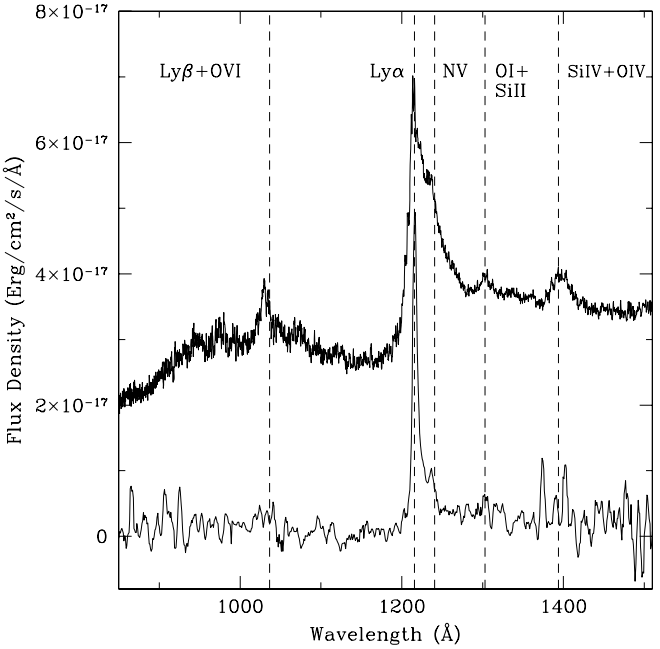

FIG. 3.—Observed optical spectrum of CXOCY J033716.7−050153 shifted into the rest frame using the best-fit redshift of 4.61. Original dispersion is 5.3 Å pixel^{-1}. The spectrum shown was boxcar-smoothed using a 5 pixel box. Resolution of the rest-frame smoothed spectrum is 5.6 Å. For comparison we also show the error-weighted average of the SDSS Early Data Release QSO spectra at $z > 4$. See (Castander et al. 2003a) for details.

[8] This sample can be found in the World Wide Web site http://www.astro.psu.edu/users/niel/papers/highz-xray-detected.dat, which is maintained by Niel Brandt and Christian Vignali.

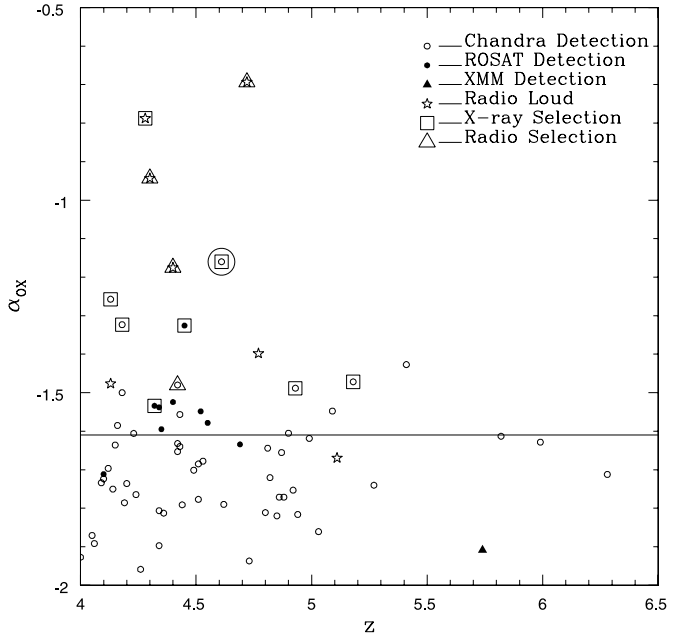

FIG. 4.—Plot of α_{ox} vs. redshift for the known sample of high-redshift AGNs detected in X-rays. Filled circles are *ROSAT* detections, empty circles are *Chandra* detections, and the filled triangle is the only *XMM-Newton* detection. Stars are radio-loud AGNs. Symbols enclosed by squares denote X-ray selection, and those enclosed by triangles denote radio selection, while no enclosing sign denotes optical selection. The horizontal line marks the position of $\alpha_{ox} = -1.61$, the average of the α_{ox} distribution. The large circle encloses the position of CXOCY J033716.7−050153.

sources have systematically higher values of α_{ox} than optically selected AGNs. This correlation is expected from selection effects; however, it should be noted that the optical luminosities of all the X-ray–selected sources are fainter than that of the least luminous optically selected quasar (with the exception of the one X-ray–selected blazar; see Fig. 5).

Recent results presented by Vignali, Brandt, & Schneider (2003) show that there is a good correlation between the UV flux characterized by the flux density at 2500 Å and the soft X-ray flux measured at 2 keV. This correlation can be expressed as $F_X \propto F_{UV}^{0.75}$. A similar result was reported in Castander et al. (2003a), in this case $F_X \propto F_{UV}^{0.55}$. This relation implies that α_{ox} should also be correlated with the UV flux (or luminosity). Figure 5 shows that optically selected AGNs are more luminous, both in the optical and the X-ray, than the X-ray–selected ones. The α_{ox} value of optically selected AGN are therefore expected to be lower as can be seen in Figure 4.

In Figure 5 we can also see that without correcting for the possible optical obscuration CXOCY J033716.7−050153 is a significant deviant from the F_X-F_{UV} relation. There are two possible explanations for this deviation: either there is significant obscuration of the optical light by dust or this a radio-loud AGN with α_{ox} enhanced by a second component, probably coronal, contributing to the X-ray emission. Strong optical variability can be ruled out using the two optical observations separated by $\sim$1 yr in the observed frame, in which the *I*-band magnitude remained almost unchanged given the error bars.

If this AGN is relatively unobscured, then its anomalous value of α_{ox}, as well as its relative optical faintness compared with other high-redshift AGNs, may be explained if the source is at the bright end of the low-luminosity AGN (LLAGN) category. Such sources are typically seen to have X-ray luminosities below about 1% of the Eddington limit (e.g., Ho 2002; Maccarone, Gallo, & Fender 2003). The mass of the central black hole would then have to be at least about $3.4 \times 10^8\ M_\odot$. Applying the black hole fundamental plane relation from Merloni, Heinz, & Di Mateo (2003),

$$\log L_R = (0.60^{+0.11}_{-0.11}) \log L_X + (0.78^{+0.11}_{-0.09}) \log M + 7.33^{+4.05}_{-4.07}, \quad (2)$$

where L_R is the radio luminosity at 5 GHz, L_X is the 2–10 keV X-ray luminosity, and M is the mass of the black hole in units of $M_\odot$, we find that the radio power is expected to be at least $f_{5\,GHz} = 31.5\ \mu$Jy. Now, if we assume instead that this is a typical AGN radiating at about 10% of its Eddington luminosity, then using the Merloni relation we get a radio flux of $f_{5\,GHz} = 5.2\ \mu$Jy. Moreover, it seems that the radio emission is quenched in AGNs accreting at about 10% of the Eddington rate (Maccarone et al. 2003), so an even lower radio flux would be expected.

Following the standard definition of radio to optical flux ratio R_{ro} given by Kellermann et al. (1989), where optical flux is defined as the flux at 4400 Å in the rest frame and radio flux is calculated at a rest-frame frequency of 5 GHz (6 cm), radio-loud sources have R_{ro} values in the range 10–1000, while for radio-quiet AGNs $0.1 < R_{ro} < 1$. With the assumption that the Eddington ratio is 1% for this AGN we obtain $R_{ro} = 15.06$, making it a radio-loud AGN. However, given the low optical luminosity, we cannot neglect the contribution of starlight from the host galaxy, in which case the value of R_{ro} computed is simply the lower limit of the

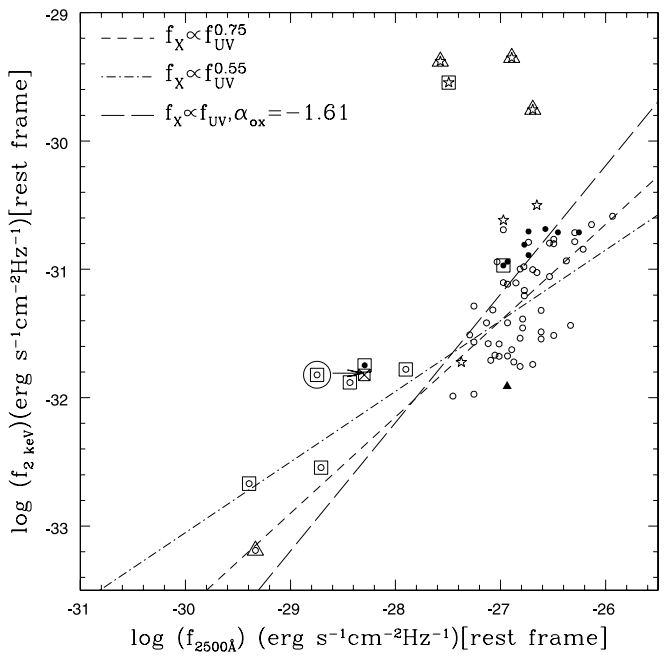

FIG. 5.—f_{2k} vs. $f_{2500\,A}$ (as defined in the text) for the known sample of high-redshift AGNs detected in X-rays. Symbols are the same as in Fig. 4. Segmented lines show the positions of the $f_X \propto f_{UV}^{0.75}$ and $f_X \propto f_{UV}^{0.55}$ correlations reported by (Vignali et al. 2003a) and (Castander et al. 2003a), respectively. The long-dashed line shows the position of sources with $f_X \propto f_{UV}$ and $\alpha_{ox} = -1.61$. The cross enclosed in a square marks the position of CXOCY J033716.7−050153 after correcting for optical obscuration, while the arrow indicates the displacement caused by this correction. The uncertainty of the X-ray flux measurement of CXOCY J033716.7−050153 is $\sim$30% and is not included for clarity.

radio-to-optical flux ratio for the AGN emission alone. Assuming an Eddington ratio of 10%, then $R_{ro} = 2.49$, which makes it a radio-quiet AGN.

According to an alternate definition of radio loudness often used for high-redshift quasars (Stern et al. 2000), to be considered radio-loud an AGN has to have a minimum 1.4 GHz specific luminosity of $L_{1.4\,\mathrm{GHz}} = 1.61 \times 10^{32}$ ergs s^{-1} Hz^{-1} (Schneider et al. 1992), which at $z = 4.61$ corresponds to a specific flux of $f_{1.4\,\mathrm{GHz}} = 0.9$ mJy, very close to the detection limit of the VLA FIRST survey. Unfortunately, the field of CXOCY J033716.7−050153 was not observed by the FIRST survey. Using the NRAO-VLA Sky Survey (NVSS; Condon et al. 1998) catalog, there were no detectable sources within a $1'$ radius. Considering that the completeness limit is 2.5 mJy, we can use this as an upper limit to the 1.4 GHz continuum emission. Then this AGN could be at most marginally classified as radio-loud.

In order to determine the amount of obscuration affecting the optical spectrum of this AGN we can compare its optical colors with a typical AGN spectrum at this redshift. The optical colors of this AGN are $V-R = 1.75 \pm 0.40$ and $V-I = 2.1 \pm 0.39$. Using the composite SDSS QSO spectrum (Vanden Berk et al. 2001) and redshifting it to $z = 4.61$, we obtain the following colors: $V-R = 1.02$ and $V-I = 1.71$, accounting for the intergalactic medium absorption using the description given in Madau (1995). If instead we use an average of all SDSS QSOs at $z > 4$, the results are very similar, finding differences $\lesssim$10%. The fact that CXOCY J033716.7−050153 is slightly redder than the average QSO at that redshift suggests that the optical spectrum is subject to some obscuration in the line of sight. In order to investigate this hypothesis, we added dust obscuration to the average spectrum following the prescription given in Cardelli, Clayton, & Mathis (1989). Given that the observed R-band flux is affected by the Lyα emission line, whose strength is highly variable from AGN to AGN, we will base our reddening estimate only on the $V-I$ color. If order to obtain a $V-I$ color of 2.1 for the redshifted composite SDSS quasar, similar to the observed value, we need to add an extinction contribution of $A_V = 0.41 \pm 0.4$ in the rest frame. Therefore, we will adopt this value to correct the observed optical fluxes for intrinsic dust extinction. It is also worth noting that the accretion disk may become cooler at lower luminosities, which would also yield redder colors.

Another typical way to calculate the amount of obscuration in the line of sight is using the X-ray spectrum. In this case, however, we do not have enough counts in the X-ray spectrum to calculate absorption directly. Also, since the observed soft X-ray band [0.5–2.0] keV translates into [2.8–11.22] keV in the rest frame, the observed X-ray spectrum is insensitive to moderate amounts of neutral hydrogen absorption ($N_{\mathrm{H}} < 10^{23}$ cm^{-2}). Using the standard dust-to-gas ratio, we can convert the optical extinction to a neutral hydrogen column density, given by $N_{\mathrm{H}} = 1.96 \times 10^{21} A_V$ cm^{-2} (Granato & Danese 1994). Then we obtain in this case that $N_{\mathrm{H}} = 8 \times 10^{20}$ cm^{-2}, implying that the X-ray spectrum is not affected by absorption in the observed energy range.

Now, correcting for the optical obscuration we compute an unobscured I magnitude of 22.52 ± 1.1. Using this value, we calculate the unobscured optical to X-ray power law slope $\alpha_{\mathrm{ox}} = -1.35$, which is now similar to the average value found for high-redshift AGNs.

As we can see in Figure 5 and already presented in Castander et al. (2003a), $f_{\mathrm{X}} \propto f_{\mathrm{UV}}^{0.55}$ is a better fit to the data if the low UV luminosity X-ray–selected AGNs are included. The values for CXOCY J033716.7−050153 are consistent with this correlation if optical obscuration is taken into account.

4. CONCLUSIONS

We present the discovery of the CXOCY J033716.7−050153, the second high-redshift X-ray–selected AGN discovered by the CYDER survey. This is a faint object in the optical. In fact, there are only two AGNs fainter at these high redshifts. The X-ray flux relative to its optical emission is unusual, having a larger value of α_{ox} than the typical AGN at high redshift. There are two effects that could bring this object into better accordance with the observed correlations for the general high-redshift population:

The first possibility is that this is a radio-loud low-luminosity AGN with a black hole of $\sim 3 \times 10^8\ M_\odot$, emitting at $\sim$1% of its Eddington luminosity. In this case the accretion disk is cooler than a typical AGN at high redshift, making the optical colors look redder. Also, the high value of α_{ox}, even taking into account the correlation with optical luminosity, can be explained by the presence of second emission component, probably coronal, which contributes to the X-ray flux measurement.

A second possibility is that this is a radio-quiet AGN emitting at an Eddington ratio of $\sim$10%, in which the optical emission is obscured by a moderate amount of dust which would imply a neutral hydrogen column density of $\sim 10^{21}$ cm^{-2}, causing the observed optical colors to be redder than the normal AGN. If this is the case, the observed value of α_{ox} is affected by the obscuration of the optical light, and after correcting for it, the corrected value agrees very well with the measurements for other high-redshift AGNs, including the observed correlation between f_{X} and f_{UV}.

Detection of a flat radio spectrum in this source above about 10 μJy would confirm the low-luminosity AGN hypothesis, while a nondetection in the radio with a sensitivity limit of a few μJy would strongly support the radio-quiet, mildly obscured AGN hypothesis.

We like to thank Meg Urry for useful discussions and the anonymous referee for helpful comments. The CYDER survey participants and especially F. J. C., E. T., and E. G. acknowledge support from Fundacion Andes. J. M. gratefully acknowledges support from the Chilean Centro de Astrofísica FONDAP 15010003. E. G. acknowledges the support of an NSF Astronomy and Astrophysics Postdoctoral Fellowship under award AST 02-01667.

REFERENCES

Anderson, S. F., et al. 2001, AJ, 122, 503
Barger, A. J., et al. 2002, AJ, 124, 1839
Brandt, W. N., et al. 2001, AJ, 122, 1
———. 2003, preprint (astro-ph/0212082)
Cardelli, J. A., Clayton, G. C., & Mathis, J. S. 1989, ApJ, 345, 245
Castander, F. J., et al. 2003a, AJ, 125, 1689
———. 2003b, AN, 324, 40
Condon, J. J., Cotton, W. D., Greisen, E. W., Yin, Q. F., Perley, R. A., Taylor, G. B., & Broderick, J. J. 1998, AJ, 115, 1693
Fan X., et al. 2003, AJ, 125, 1649

Granato, G. L., & Danese, L. 1994, MNRAS, 268, 235
Hasinger, G. 2002, preprint (astro-ph/0202430
Henry, P. J., et al. 1994, AJ, 107, 1270
Ho, L. 2002, ApJ, 564, 120
Kaspi, S., et al. 2000, AJ, 119, 2031
Kellermann, K. I., Sramek, R., Schmidt, M., Schaffer, D. B., & Green, R. 1989, AJ, 98, 1195
Maccarone, T. J., Gallo, E., & Fender, R. 2003, MNRAS, 345, L19
Madau P. 1995, ApJ, 441, 18
Merloni, A., Heinz, S., & Di Matteo, T. 2003, MNRAS, 345, 1057
Schmidt, M., 1963, Nature, 197, 1040
Schneider, D. P., van Gorkom, J. H., Schmidt, M., & Gunn, J. E. 1992, AJ, 103, 1451
Schneider D. P., et al. 1998, AJ, 115, 1230
———. 2002, AJ, 123, 567
———. 2003, AJ, 126, 2579
Silverman, J. D., et al. 2002, ApJ, 569, L1
Spergel, D. N., et al. 2003, ApJS, 148, 175
Stern, D., Djorgovski, S. G., Perley, R. A., De Carvalho, R. R., & Wall, J. V. 2000, AJ, 119, 1526
Treister, E., et al. 2004, in preparation
Vanden Berk, D. E., et al. 2001, AJ, 122, 549
Vignali, C., Brandt, W. N., & Schneider, D. P. 2003, AJ, 125, 433
York, D. G., et al. 2000, AJ, 120, 1579
Zickgraf, F. J., et al. 1997, A&A, 323, L21